Experimental Investigation of a Superconducting Switch at Millimetre Wavelengths

Boon-Kok Tan, Ghassan Yassin, *Member, IEEE,* Ernst Otto, and Leonid Kuzmin

***Abstract*—We present preliminary measured responses of a planar superconducting on/off switch operating at millimetre wavelengths. The superconducting switch, comprising three niobium nitride (NbN) bridges, is deposited across the slotline section of a back-to-back unilateral finline. The transmission characteristics of the superconducting switch illuminated by a millimetre source was measured using a superconductor-insulator-superconductor (SIS) tunnel junction as direct detector. The NbN bridges were switched from the superconducting state to the normal state by passing current through the bridges with magnitude that exceeds its critical current value. With this arrangement, we have measured a typical switching dynamic range of approximately 10 dB across the 205−240 GHz band, with the highest dynamic range of ∼20 dB at 230 GHz. This demonstrated the successful operation of the multiple NbN bridges as a planar superconducting on/off switch.**

***Index Terms*—Modulators, Millimeter astronomy, Millimeter wave devices, Millimeter wave technology, Terahertz switch**

I. Introduction

A high speed switch that can be used to modulate millimetre and sub-millimetre signals is an important component for constructing a phase modulator that is essential for an ultra-sensitive pseudo-correlation polarimeter to measure the polarisation of the B-mode Cosmic Microwave Background signals [1]. Phase modulation does not only reduce the $1/f$ noise substantially, but also allows the measurement of the Stokes parameters without having to move the polarimeter optics. A high performance phase switch will have the following features:

- fast switching rate, which can be necessary if many channels are switched at different rates,
- high dynamic range,
- low dissipation loss, and
- highly integrated to prevent systematics and allow repeatable production.

Three major techniques that have been considered for modulating the polarisation signal in various B-mode instruments are 1) the use of a rotating half-wave plate in front of the detector array, 2) integrating rotating waveguide sections in individual polarisation channels, and 3) employment of Faraday rotator ferrite rods. The first method is relatively simple to implement as it only requires a single rotating quasioptical plate for the whole instrument. However, it could impart polarisation systematics caused by the anisotropies of the plate material, and the scattering aperture of the plate could potentially degrade the optical performance of the instrument. The rotating waveguide technique requires moving parts in the construction of the modulator, in particular it requires a large number of cryogenic motor and a large number of highly accurate movable waveguide sections at the higher end of the millimetre spectrum. The third option has been considered attractive since it requires no mechanical moving parts and has since been implemented in instrument like BICEP. However, it was found that Faraday rotators are difficult to mass produce and they suffer from significant RF losses as well.

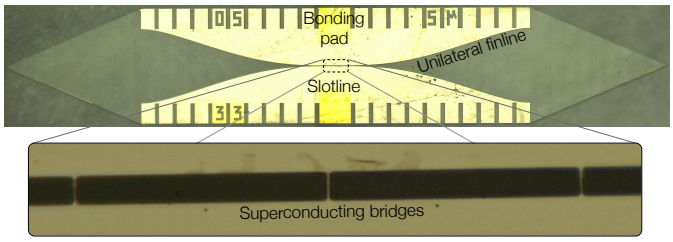

Fig. 1. A planar superconducting switch chip comprising three NbN bridges deposited across the slotline section of a back-to-back unilateral finline taper.

A potentially much more efficient and elegant alternative is to use the pseudo-correlation polarimeter in conjunction with a planar circuit phase switch [2]. They are relatively easy to fabricate at high frequencies, and do not require any rotating components or obstacles that introduce polarisation systematic errors. An additional important advantage of a planar switch design is that it allows the modulator to be easily integrated into the detector circuit, offering a compact and low power consumption solution, and therefore enabling the construction of a large format focal plane array.

The planar switch we consider here comprises three narrow superconducting strips fabricated across a slotline fed directly by two back-to-back unilateral finline tapers [3], as shown in Fig. 1. These bridges were formed using high normal resistance niobium nitride (NbN) film of 50 nm thick. Each NbN bridge is 0.5 μm wide and 5 μm long, and are separated by a 50 μm long slotline. The whole structure including the finline tapers are deposited on a 100 μm thick quartz substrate [4]. The planar switch presented here was designed to operate in the frequency range of 180–260 GHz.

The superconducting switch chip was positioned in the E-plane of a rectangular waveguide, fed by a feed horn as shown in Fig. 2. The RF signal injected from one end of the chip was either transmitted towards the other end of the chip or reflected back to the input port, depending on the state of

B-K. Tan and G. Yassin are with the Department of Physics (Astrophysics), University of Oxford, Denys Wilkinson Building, Keble Road, OX1 3RH, Oxford, UK. E-mail: tanbk@astro.ox.ac.uk

E. Otto and L. Kuzmin are with the Department of Microtechnology & Nanoscience, Chalmers University of Technology, S-41296 Gothenburg, Sweden.

Manuscript received XXXX XX, 2015; revised XXXX XX, 2015.

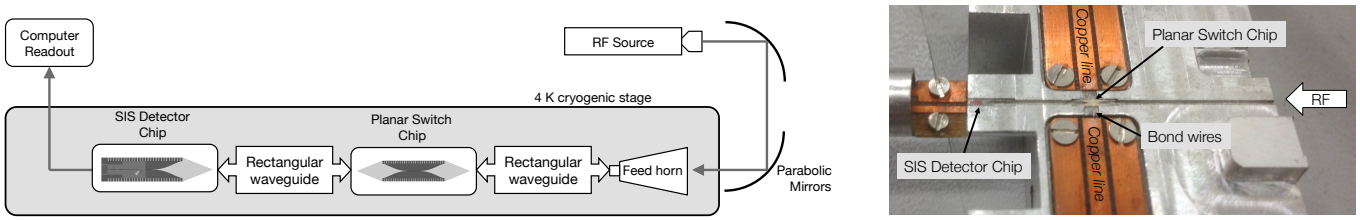

(a) (b)

Fig. 2. (a) Experimental setup for measuring the response of the superconducting on/off switch using an SIS device as direct power detector. (b) Both the SIS detector chip and the switch chip are supported across the E-plane of a rectangular waveguide via the grooves in the waveguide wall. Two copper lines and bond wires are used to supply the bias current that switch the bridges between the superconducting and the normal state. The RF signal from the feed horn is coupled to the slotline and the bridges via a unilateral finline taper, and re-radiated towards the SIS detector chip via a similar finline taper.

the switch. A superconductor-insulator-superconductor (SIS) device designed to operate in the same frequency range was placed after the switch chip to detect the transmitted RF power. The detail of the SIS detector chip can be found in [5]. Both the switch and the SIS detector chip were located in an aluminium split block, which was mounted on the cold plate of a Gifford-McMahon (GM) cooler to cool both the chips down to cryogenic temperature (4.2 K).

The NbN bridges were made to alternate between the superconducting (off) and the normal (on) states by applying a bias current along the parallel-bridges through aluminium bond wires, causing them to become normal when the bias current exceeds the critical current (I_c) value. In this arrangement, the incoming RF signal sees two substantially different complex impedance states, hence will either pass through the transmission line with negligible loss or reflected back with high return loss [6]. The response of the switch is obtained by comparing the tunnelling current through the SIS device at each state.

II. Theoretical Model

The impedance of a superconducting strip is given by $Z_L = R_s + i\omega L$, where R_s is the resistive part of its surface impedance, and $L = L_g + L_k$ where L_g is the geometric inductance and L_k is the kinetic inductance of the bridges [2]. The kinetic inductance has a significant value only in the superconducting state and in that case $R_s \approx 0$, whereas in the normal state $R_s = R_N$, its thin film normal resistance. The value of these parameters can be approximated by:

$$R_N = \frac{\rho l}{wt}, \tag{1a}$$

$$L_g \cong 0.2l\left[\frac{1}{2} + \ln\left(\frac{2l}{w+t}\right) + 0.11\left(\frac{w+t}{l}\right)\right]\mu\text{H}, \tag{1b}$$

$$L_k = \mu_0 \frac{l\lambda_L}{w}\coth\frac{t}{\lambda_L}, \tag{1c}$$

where ρ is the resistivity of the superconductor, λ_L is the London penetration depth, and w, l and t is the width, length and thickness of the superconducting strip respectively. For an RF signal at an angular frequency of $\omega = 2\pi f$, the total impedance at superconducting and normal states are therefore:

$$Z_{off} = i\omega(L_k + L_g), \quad \text{and} \tag{2a}$$

$$Z_{on} = R_N + i\omega L_g, \tag{2b}$$

where Z_{off} and Z_{on} are the impedance of the strip operating as a switch at the superconducting and the normal states respectively.

Using a simple model where a transmission line is shunted by a single load resistance to represent the impedance of a NbN bridge, one can show that the voltage transmission (τ) and reflection (Γ) coefficient are given by

$$\tau = \frac{2Z_L}{Z_0 + 2Z_L} \quad \text{and} \quad \Gamma = \frac{-Z_0}{Z_0 + 2Z_L}, \tag{3}$$

where Z_0 is the characteristic impedance of the transmission line and Z_L is the load impedance of the bridge. The dynamic range of the switch is therefore determined primarily by the ratio between $Z_L = Z_{on}$ and $Z_L = Z_{off}$. In other words, an ideal switch would have high normal state resistance and low superconducting kinetic inductance. In principle, this condition can be achieved by employing highly resistive superconductors such as niobium titanium nitrid (NbTiN) or NbN films. However, for a switch that is designed to operate at high frequencies, the total surface impedance induced by the kinetic inductance of the bridge could be very high, approaching the value closed to R_N, thereby reducing significantly the dynamic range of the switch. This is especially severe in our case where the switch is designated to operate at higher end of the millimetre wavelength spectrum.

In order to alleviate this problem, we employ a multiple bridge design that allows us to alter the total impedance of the switch seen by the incoming millimetre signal at both normal and superconducting states, giving us a degree of freedom in selecting the optimum operating point of the switch. This is illustrated in Fig. 3 where we show an example of how the power transmission changes with the surface impedance of a superconducting strip across a slotline. It can be seen that due to this nonlinear relation, the dynamic range of the switch can be improved by several orders of magnitude if the surface impedance value can be reduced by half. This insight has therefore led us to change our initial design strategy which was based on a single bridge with high normal resistance superconductor to three NbN bridges in parallel formed using a thicker film which reduces R_N, but more importantly produces a much smaller kinetic inductance L_k value[1] (see Eq. 1).

In order to calculate the dynamic range of the triple-bridge design, we use a triple cascaded loads model shown in Fig. 4.

[1]For a superconducting strips, its normal resistance decreases linearly with the film thickness, but the surface resistance decreases exponentially.

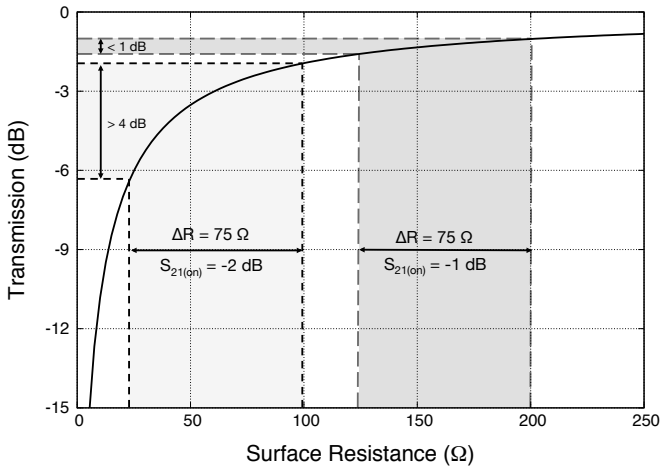

Fig. 3. The nonlinear relation between the surface resistance of a superconducting strip deposited across a slotline and its power transmission characteristic, plotted using Eq. 3.

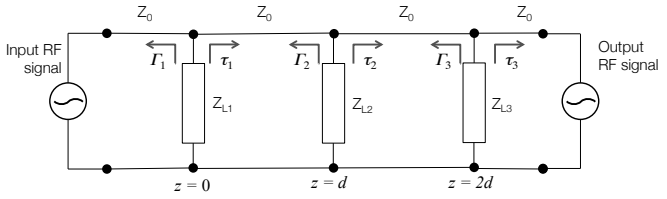

Fig. 4. A simple transmission line model depicting a transmission line shunted with three loads representing the impedances of the NbN bridges.

To find the total voltage transmission coefficient from the input to the output port, we need to take into account the interactions between the loads. For example, to calculate τ_1 at $z = 0$, we first obtain the effective input impedance of Z_{L2} and Z_{L3} transformed by a transmission line of length d and $2d$ respectively, where d is the distance between two bridges. The input impedance at a distance l from the load can be found by using

$$Z'_L(l) = Z_0 \frac{1+\Gamma(l)}{1-\Gamma(l)}, \quad \text{where} \tag{4}$$

$$\Gamma(l) = \frac{-Z_0}{Z_0 + 2Z_L} e^{-i2\beta l}. \tag{5}$$

The total impedance seen by the incoming signal at $z = 0$ is therefore the product of three parallel loads. Replacing $Z_L = Z_{z=0}$ in Eq. 3, and repeat the same calculation for $z = d$ and $z = 2d$, we can therefore obtain the output voltage transmission and reflection coefficient for the complete three bridges model. For example, using $\rho = 140$ $\mu\Omega$cm, $\lambda_L = 200$ nm, $d = 50$ μm and $Z_0 = 75$ Ω for a 5 μm wide slotline on a 100 μm thick quartz, we estimate that the power ratio $D_P = \tau_{on}^2/\tau_{off}^2 \approx 20$ dB at 180 GHz and gradually dropping to approximately 12 dB at 260 GHz, as shown in Fig. 5. This gradual decrease is caused by the increase in the kinetic inductance of the bridges as the frequency becomes higher.

This transmission line model does not take into account the fringing effect of the various electromagnetic structures of the switch, especially the slotline. In practice, the field strength

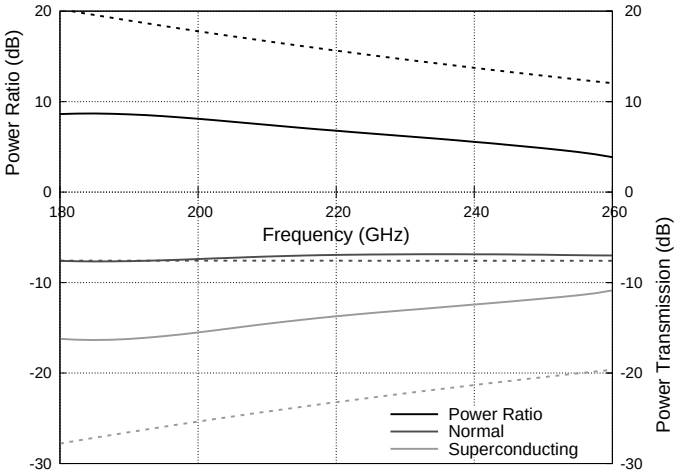

Fig. 5. Dynamic ranges (black) and power transmissions (dark grey for normal state and light grey for superconducting case) of a slotline shunted with three NbN bridges separated by 50 μm slotlines. The solid lines represent the predictions from HFSS model, while the dashed lines show the calculated performances from the transmission line model.

of a slotline is not perfectly confined between the two parallel electrodes, since a small part of it is fringed above and below the slotline. Although the fringing field contains only a small percentage of the transmitted power, it does have significant impact especially when the superconducting bridges should short the slotline substantially. A more accurate method to simulate the behaviour of the switch therefore is to use a 3-D electromagnetic simulator to fully model the structure of the switch. In our case, we used Ansys High Frequency Structure Simulator (HFSS) which includes the fringing and the superconductivity effect. The complex conductivity of the NbN film was calculated using the standard Mattis-Bardeen equation in the extreme-anomalous limit [7], and applied to a Perfect Electrical Conductor (PEC) medium in the HFSS model using sextic polynomial functions.

The HFSS simulated results are plotted in Fig. 5, along with the plots made using the transmission line model. Notice that the dynamic range computed by HFSS is about 10 dB lower than the values obtained by the transmission line model as a result of HFSS taking into account the increase in the transmitted power, due to fringing, when the bridges are superconducting.

III. Preliminary Experimental Results

In Fig. 6, we show the DC current-voltage (IV) curves of the SIS device measured at 216 GHz and 230 GHz, respectively. The grey lines shows the pumped IV curves when the switch is biased below I_c, and the black lines for the case when the switch is not superconducting. The changes in the level of the tunnelling current across the first photon step (approximately from 2.0–2.5 mV) are significant. When the bridges are superconducting, they effectively short (apart from the small value due to the inductance) the transmission line. The RF power coupled to the SIS devices is therefore significantly attenuated. On the other hand, when the bridges are biased above I_c, the complex impedance of the bridges

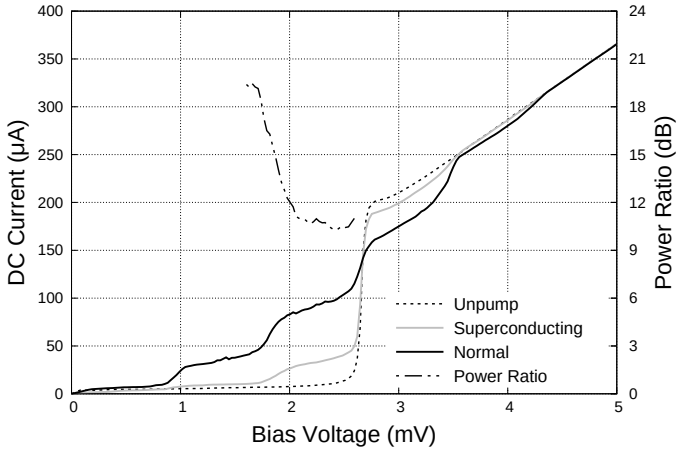

(a) $f_{RF} = 216$ GHz

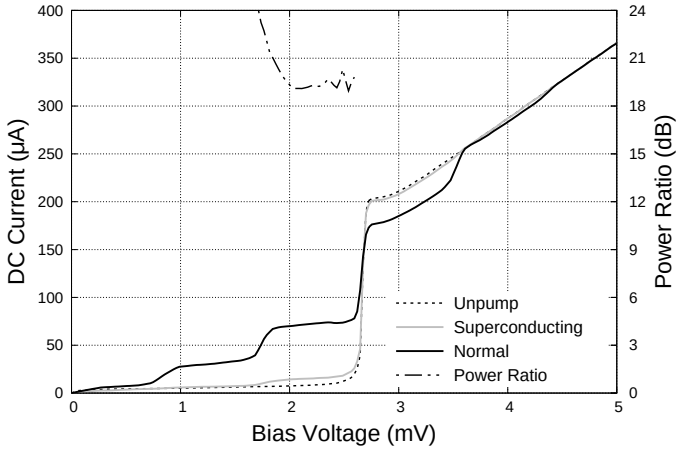

(b) $f_{RF} = 230$ GHz

Fig. 6. The normalised DC pumped IV curves of the SIS devices under the illumination of the RF source. The grey curves show the tunnelling current measured across the SIS device when the bridges are superconducting, and the black curves for the bridges biased to the normal state. The unpumped curves are shown as dashed line for reference. The power ratio between the switching states are shown above the IV curves as dot-dot-dash line.

becomes high and the incoming signal therefore pass through with small loss, resulting in substantial increase in the power detected by the SIS device.

Note however that, it is important to bias the bridges just above the critical current but not much higher, because excessive bias current through the bridges could potentially heat up the transmission line and therefore increase the conduction loss. In Fig. 7, we plot the measured amplitude of the tunnelling current through the SIS device (biased at 2.4 mV) against the switch's bias current. The increase in the tunnelling current at I_c is obvious at approximately 300 μA. However, if the bias current is increased beyond I_c, one notices that it begins to drop gradually. We attribute this to the effect of heating caused by the excessive current flowing through part of the slotline section where the bridges are located, causing the transmission line to turn normal, thereby increasing the conduction loss. At first, one could argue that by supplying a bias current way beyond the critical current (says I_{max}), all the incoming power would be absorbed by the transmission line,

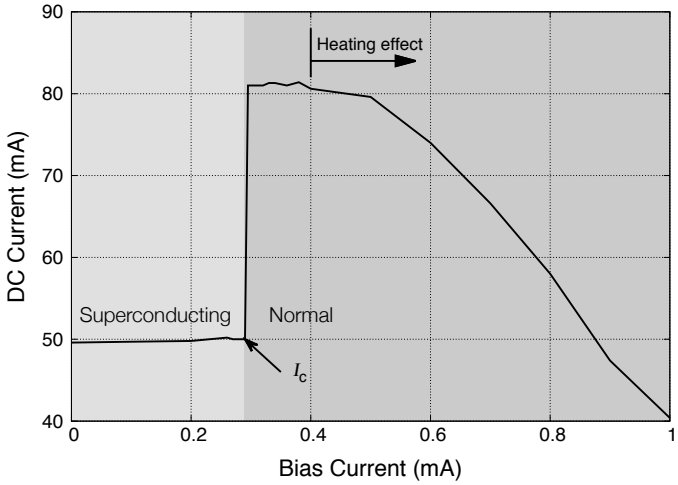

Fig. 7. Graph showing the onset of increase in tunnelling current at I_c and the gradual decrease of the tunnelling current due to the heating effect increasing the conduction loss of the transmission line.

and therefore by alternating between I_c and I_{max}, the dynamic range of the switch could be very high. This however is only true for applications that do not require the use of the reflected power, for example in the case where the switch is used as a switching modulator. But for applications where reflected power is required, such as when the devices are used in a phase switch circuit for CMB polarimeter, the conduction loss needs to be minimised.

Referring to Fig. 6, we find that the ratio of power transmission between the switch-on and switch-off state is approximately 11 dB at 216 GHz and $\sim$ 20 dB at 230 GHz. This switching ratio is measured as the change in the level of tunnelling current with reference to the leakage current measured from the unpumped curve. It is worthwhile noting that the level of pumping was determined by gradually increasing input power of the RF source until it reached the maximum power ratio value. We found that this often results in a tunnelling current of approximately half the critical current of the SIS device at the first photon step when the switch is in the normal state, as shown in Fig. 8.

In Fig. 9, we show the measured responses of the three-bridges switch in the frequency range of 205–240 GHz (range which is limited by the power availability from our RF source). Comparing these with the values computed from both the transmission line method and HFSS simulations from Fig. 5, it can clearly be seen that the dynamic range varies periodically with frequency which is unexpected from both models. We also noticed that while the average dynamic range agrees reasonably well with simulations, the details are quite different. The predicted values could disagreed by as much as 10 dB in the extreme case.

To further understand the interaction between the switch and the SIS devices, and to estimate the power coupling behaviour of the SIS detector, we used SuperMix, a quantum mixing software package developed at Caltech [8], to reproduce the pumped IV curves. The HFSS calculated scattering parameters of both the switch and the SIS detector chip were imported into SuperMix to form a model of our experimental setup. Since

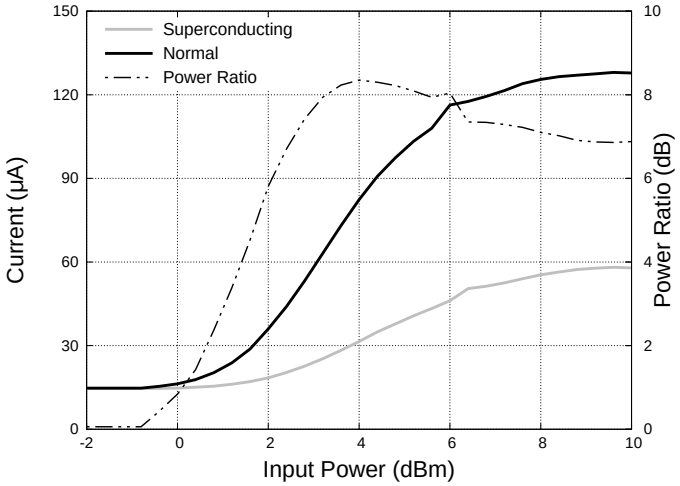

Fig. 8. The amplitude of the SIS tunnelling current plotted against the input power from the RF source for both the superconducting (dark line) and normal (grey line) cases. The power ratio between the two switching states is plotted as the dot-dot-dash line.

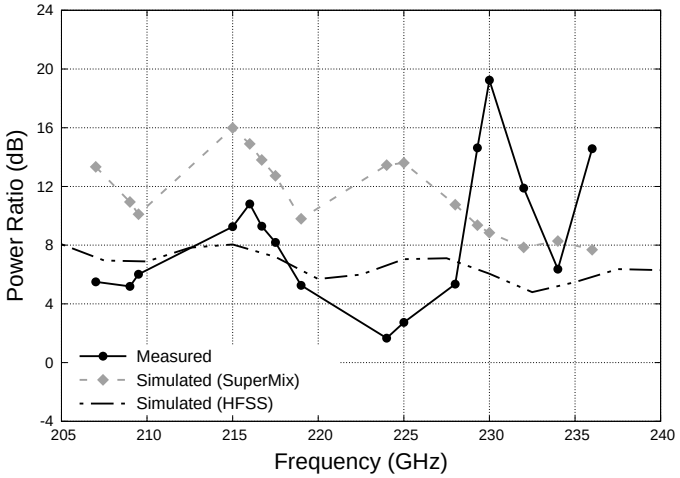

Fig. 9. The power ratio variation of the switch measured across the designated frequency range (black curve), and the SuperMix predicted power ratio plotted in grey.

the RF quasioptical components such as the millimetre horn and the parabolic reflectors were not included in the model, we estimated the RF input power by calibrating the pumped current at the normal state to the measured pumped level. The scattering parameter of the normal switch is then replaced in the SuperMix circuit with a superconducting switch to calculate the pumped level at the superconducting state, and thereby to estimate the power ratio between the two states. The advantage of using the SuperMix model is that it benefits from both the electromagnetic rigour of HFSS and the accuracy in calculating the power coupling to the SIS device. Initially, we found that this theoretical model did not produce the frequency periodic variations observed by the experiment. This was quite puzzling since the SIS device's coupling bandwidth was designed to cover a larger frequency range than that of the measurement and that was verified in a separate experiment.

We therefore were led to conclude that there exist an effect that influences our measurements but is not included in our simulations. One possibility we considered was that the incoming RF signal could influence the kinetic inductance of the bridge by Cooper pairs breaking. Another obvious possibility was the existing of standing waves between the switch chip and the SIS detector chip, since both were fabricated on 100 μm quartz substrate and the detector chip did not have a matching notch. While we have made sure that these substrates do not overload the waveguide individually, standing waves can still be established by multiple reflections.

To verify the influence of standing waves, we included the front end of the detector chip (i.e., the finline part) into our switch model in the HFSS environment. The HFSS predicted dynamic range of this model is shown in Fig. 9 as the dot-dot-dash curve. It can be clearly seen that a periodic dependence does exist now in the simulation, albeit it only agrees with the measurements at the low frequencies side. We next exported the new HFSS model into SuperMix via scattering parameters. The SuperMix calculated results are also plotted in Fig. 9, as the grey curve. As expected, similar periodic frequency variations are obtained, but the average simulated dynamic range is higher than the measured results. Standing waves between the two chips therefore seem to influence the measurements significantly, although it might not account for the results obtained at all frequencies, in particular around 225 GHz. Considering that standing waves can arise from other aspects such as chips misalignment, they must be considered as a strong candidate for the discrepancies between simulations and measurements.

Despite these discrepancies, we have demonstrated experimentally that the multiple bridge design can be used as an efficient on/off switch in millimetre circuits. Work is in progress to minimise the measurement systematic errors, in particular the interaction between the switch and the detector chips by improving the matching of the chips to the waveguide; and to reduce the joule heating of the chip via a better cooling mechanism. We are also in the process of modifying the design to improve the performance of the switch. One of the fundamental disadvantage of the current design is that although the dynamic range is improved by reducing the total normal resistance of the switch, it decreases the power transmission when the switch is at the normal state. This is demonstrated graphically in Fig. 3. As the normal resistance of the switch is reduced by half, the insertion loss decreases from approximately -1.5 dB to -2 dB, thereby increasing the RF loss of the signal. This weakness can potentially be overcame by using a resonant bridge architecture. The detail of this resonance design can be found in [9].

IV. Conclusion

We have demonstrated the successful operation of a planar on/off switch comprising three NbN bridges deposited across the slotline section of a back-to-back finline chip. The NbN bridges were made to alternate between the superconducting and the normal state by passing a bias current whose magnitude is higher than its critical current of the bridges. Using an SIS device as a direct power detector, we have measured a switch dynamic range about 10 dB across the frequency band

when the switch was biased from superconducting to normal state. Although the frequency dependent variation of the power ratio measured for this device are yet to be fully understood, we have shown that the NbN multiple bridges switch does indeed operate as a superconducting switch with high dynamic range. Work is in progress to improve the measurement method by minimising the standing waves between the switch and the detector chips, and to increase the dynamic range by tuning out the kinetic inductance entirely using a twin-bridge structure.

REFERENCES

[1] P. K. Grimes, G. Yassin, L. S. Kuzmin, P. D. Mauskopf, E. Otto, M. E. Jones, and C. E. North, "Investigation of planar switches for large format CMB polarization instruments," in *Society of Photo-Optical Instrumentation Engineers (SPIE) Conference Series*, ser. Society of Photo-Optical Instrumentation Engineers (SPIE) Conference Series, vol. 6275, Jul. 2006.

[2] G. Yassin, L. S. Kuzmin, P. K. Grimes, M. Tarasov, E. Otto, and P. D. Mauskopf, "An integrated superconducting phase switch for cosmology instruments," *Physica C Superconductivity*, vol. 466, pp. 115–123, Nov. 2007.

[3] L. Kuzmin, M. Tarasov, É. Otto, A. Kalabukhov, G. Yassin, P. Grimes, and P. Mauskopf, "Superconducting subterahertz fast nanoswitch," *Soviet Journal of Experimental and Theoretical Physics Letters*, vol. 86, pp. 275–277, Oct. 2007.

[4] B.-K. Tan, G. Yassin, E. Otto, and L. Kuzmin, "Experimental Investigation of a 220 GHz Planar Multiple Bridges Superconducting Switch," in *Proceeding of the 8th UK, Europe, China conference on Millimetre Waves and Terahertz Technologies.*, Sep. 2015.

[5] J. Garrett, B.-K. Tan, F. Boussaha, C. Chaumont, and G. Yassin, "A 220 GHz Finline Mixer with Ultra-Wide Instantaneous Bandwidth," in *Twenty Sixth International Symposium on Space Terahertz Technology*, Mar. 2015.

[6] B.-K. Tan, G. Yassin, L. Kuzmin, E. Otto, H. Merabet, and C. North, "A Superconducting Millimetre Switch with Multiple Nano-Bridges," in *Twenty Fifth International Symposium on Space Terahertz Technology*, Apr. 2014.

[7] D. Mattis and J. Bardeen, "Theory of the anomalous skin effect in normal and superconducting metals," *Physical Review*, vol. 111, no. 2, p. 412, 1958.

[8] J. Ward, F. Rice, G. Chattopadhyay, and J. Zmuidzinas, "Supermix: A flexible software library for high-frequency circuit simulation, including sis mixers and superconducting elements," in *Proceedings, Tenth International Symposium on Space Terahertz Technology*, 1999, pp. 269–281.

[9] B.-K. Tan, G. Yassin, E. Otto, and L. Kuzmin, "Investigation of the Dynamic Range of Superconducting Nano-Bridge Switches," in *Twenty Sixth International Symposium on Space Terahertz Technology*, Mar. 2015.

Boon-Kok Tan received the B.Eng. degree in Electrical and Electronic Engineering and the M.Eng. degree in Solar Engineering from University of Technology Malaysia, in 2001 and 2003, respectively. He received his D.Phil. degree in Astrophysics from University of Oxford, United Kingdom, in 2012.